Journal of Inorganic and Organometallic Polymers and Materials (2018) 28:1942–1952
https://doi.org/10.1007/s10904-018-0862-3

The Mixed Contribution of Ionic and Electronic Carriers to Conductivity in Chitosan Based Solid Electrolytes Mediated by CuNt Salt

Shujahadeen B. Aziz[1,2]

Received: 8 February 2018 / Accepted: 27 April 2018 / Published online: 28 April 2018

Abstract
This work shows the contribution of both ionic and electronic conductivities in chitosan (CS) based solid polymer electrolytes incorporated with various amounts of copper nitrate (CuNt). The samples were prepared using solution cast technique. The second semicircles at intermediate frequency in impedance plots were observed. Surface plasmonic resonance (SPR) was illustrated from the UV–Vis spectrophotometry, where broad peaks at 702 nm were obtained as an evidence for nanoparticles formation. The second semicircles in the impedance plots and the distinguished SPR peaks have revealed the contribution of electronic conductivity in CS:CuNt based polymer electrolytes. The same trend of UV–Vis spectra at different temperatures reveals that CS:CuNt polymer electrolyte is thermally stable. The presence of electronic conductivity is the main shortcoming of copper ion conducting solid polymer electrolytes. The role of lattice energy of the copper salts on electrical properties and morphological (SEM) appearance was discussed. The TEM image shows Cu nanopartciles with various sizes. A stable SPR peak and vanishing of second semicircle at high temperatures reveals the stability of copper ion conducting chitosan based polymer electrolytes. The pattern of DC conductivity and dielectric constant as a function of salt concentration are almost found to be similar. Both estimated DC conductivities from AC spectra and those calculated from impedance plots are shown to be comparable. Highest DC conductivity of 3.65×10^{-5} S/cm has been achieved for the sample incorporated with 21 wt% of CuNt. The high value of dielectric constant at low frequency can be ascribed to electrode polarization. Electric modulus parameters are studied to understand the relaxation process. Two semicircles in Argand plots were separated.

Keywords Chitosan electrolyte · Copper nanoparticles · UV–Vis · Impedance plots · SEM · Electrical properties · Lattice energy of salts

1 Introduction

Solid polymer electrolytes have attracted attention of many researchers. This is owing to the wide applications, for instance fuel cells, super capacitors, sensors and electrochromic windows [1]. Polymer electrolytes consist of polymer-salt complexes that are formed by salt dissolving process in matrices comprising from polymer containing hetero-atoms, such as O, N and S [2]. Polymer electrolytes have relatively high ionic conductivity in their solid phases, which is a desired property. Moreover, they have more additional characteristics, such as processability, flexibility, light weight, elasticity and transparancy [3]. Nowadays, the main focus is to develop portability, wearability and flexibility of electronic devices. Among them, portable solid-state electrolytes are mainly important in developing wearable electronics. The interface region between ionic conducting media and solid electrode is provided by a piece of solid-state electrolytes [4]. The necessity of minimizing the influence of hazardous materials on human environment has encouraged scientists to develop and synthesize environmentally and friendly green materials instead. To achieve this goal, the appropriate alternatives for long-term uses as electrolytes are the usage of natural biopolymers owing to their biodegradability property [5]. Numerous natural biopolymers are now available and in uses, for example, starch, cellulose, chitosan,

✉ Shujahadeen B. Aziz
shujaadeen78@yahoo.com; shujahadeenaziz@gmail.com

[1] Advanced Polymeric Materials Research Lab., Department of Physics, College of Science, University of Sulaimani, Qlyasan Street, Sulaimani, Kurdistan Regional Government, Iraq

[2] Komar Research Center (KRC), Komar University of Science and Technology, Sulaimani 46001, Kurdistan Regional Government, Iraq

carrageenan and agarose [6, 7]. Electrolytic polymers have a capability to dissolve inorganic salts resulting from a direct interaction of their functional group-containing oxygen and nitrogen with cations and anions. Therefore, the widespread uses of natural solid biopolymer electrolytes (SBEs) keep our environment free of toxic materials [6]. Furthermore, those kinds of polymers have more additional characteristics, such as relatively low cost and high ability in solubilization of chemicals and forming a mechanically durable film. Chitosan (CS) is considered as one of the most common and promising natural biopolymers [5]. Former studies have emphasized that the two functional groups; hydroxyl, OH and amine, NH_2, have enabled chitosan to solubilize doping salts [8–11]. Chitosan is the derivative obtained from dissolving N-deacytelated chitin in dilute acids. It exhibits a high mechanical strength and also chemical and thermal stability up to 200 °C [12]. Recent studies have revealed that CS biopolymer is the subject of intensive study for the preparation of CS based hydrogels. CS is highly negatively charged and thus it can attract free cations from the medium and successfully used to produce CS-based hydrogel, which is widely used in tissue engineering [13]. CS Hydrogels are extremely suitable for a variety of applications in the pharmaceutical and medical industry. Since they are capable of retaining large amounts of water and because of their soft and rubbery consistence, they closely resemble living tissues [14]. Sun et al., have found that the CS–Ag hydrogel exhibits versatile and multifunctional properties. They have achieved the fact that CS-based biopolymers are very useful natural resources for the design of advanced soft materials, which are crucial for applications in smart devices, logic gates, sensors, and in antibacterial gel membranes [15]. A pure chitosan membrane is an insulator; however, it has an ability to host ionic conductivity when solvated with lithium salts [16]. Most of the modern portable rechargeable batteries available today in the market are lithium based batteries. It is well-known that lithium compounds are highly reactive and toxic particularly in open humid environments. Alternatively, several dry polymer electrolytes containing divalent cations, for instance Mg^{2+}, Zn^{2+} and Cu^{2+} have been studied recently. Divalent cations are relatively cheaper, abundance naturally, non-reactive, and environmentally friendly. From Faraday point of view, divalent cations displace twice as much more charge as mono-valent cations [17]. Previous studies have showed that copper ion conducting polymer electrolytes in solid polymer batteries can be used instead of other divalent-based electrolytes if they have no desirable electronic conductivities [18, 19]. Compared to the metallic lithium as an anode material in solid state batteries, copper shows several benefits, such as less expensive and environmentally stable [18]. From the above survey, it is understood that polymer electrolytes must only exhibit ionic conductivity instead of any electronic conductivity. In our former works, it is confirmed that silver ion undergoes reduction to silver in the form of nanoparticles in chitosan based solid electrolytes [20–25]. In addition of that the reduction of silver ions to nanoparticles has been shown to increase with increasing temperature in chitosan based solid polymer electrolytes mediated by silver triflate ($AgCF_3SO_3$) salt [20, 21, 25]. Furthermore, Patel et al., have reported the reduction of silver ions (Ag^+) to silver nanoparticles (Ag^o) through the heavy ion irradiation of chitosan based electrolytes mediated by silver nitrate ($AgNO_3$) [26]. They have observed significant influence of silver ion reduction on electrical and optical properties of chitosan polymer films. Perera et al., [18] have reported the contribution of electronic conductivity through measuring transference number in copper ion conducting solid polymer electrolytes based on polyacrylonitrile polymer. In the present work, chitosan based solid electrolytes incorporated with divalent salts, such as CuNt, was studied. The optical and morphological properties were examined with UV–Vis spectroscopy, scanning electron microscope (SEM) and transmission electron microscope (TEM) techniques, respectively. The impedance data results and UV–Vis absorption spectra have revealed the formation of metallic copper particles, which in turn resulted in the electronic conductivity.

2 Experimental method

2.1 Materials and sample preparation

Chitosan (CS) from crab shells (≥ 75% deacetylated, average molecular weight 1.1×10^5 g/mol) and $Cu(NO_3)_2$ (CuNt) salt materials used in this work were provided by Sigma-Aldrich. The above have been used as the raw materials. One gram of chitosan (CS) powder was dissolved in 100 ml of 1% acetic acid. The solution was stirred using a magnetic stirrer for more than 24 h at room temperature until the polymer was completely dissolved and clear viscose solutions were obtained. For the chitosan solution, various amounts of CuNt was added separately with continues stirring to prepare CS:CuNt electrolyte solution. The color of the CS:CuNt was appeared to be greenish which is related to the formation of Cu^o nanoparticles. The polymer electrolyte samples were coded as CSSPE1, CSSPE 2, CSSPE 3 and CSSPE 4 for CS incorporated with 7, 14, 21, and 28 wt% of CuNt, respectively. After casting in different Petri dishes, the solutions were left to dry at room temperature for films to form. The films were transferred into desiccators for continuous drying. This procedure produces solvent-free films.

2.2 Characterization Techniques

The electrical properties of the samples were measured using HIOKI 3531 Z Hi-tester. Sample preparations were performed by cutting nanocomposite solid polymer films into small discs with 2 cm in diameter and then sandwiched between two stainless steel electrodes. The impedance measurements were carried out within the frequency range of 0.05–1000 kHz. The UV–Vis spectra of the CS:CuNP films have been recorded using a Jasco V-570 UV–Vis–NIR spectrophotometer (Japan, Jasco SLM-468) in the absorbance mode. The SEM and TEM images were taken using the FEI Quanta 200 FESEM scanning electron microscope and Transmission electron microscope, respectively. The SEM was operated using a LEO LIBRA instrument with accelerating voltage of 120 kV. For TEM measurement, a drop of chitosan: CuNP solution containing Cu nanoparticles was placed on a carbon-coated copper grid. The excess solution was then removed using filter paper and the grid was left at room temperature to dry prior being imaged.

3 Results and Discussion

3.1 Impedance Study

Figure 1 illustrates the impedance plots for CS:CuNP solid electrolyte samples. Two semicircles are the main features of impedance spectra; one at the high frequency region and the other at the intermediate one. The first one at the high frequency region indicates the bulk conductivity [19], whereas the second one at the intermediate region is evidenced the formation of nanoparticles. In our previous works, we have successfully used impedance plots to detected the formation of silver nanoparticles in chitosan based solid electrolytes [21, 25, 27]. It is worth-mentioning that the investigation Cu-nanoparticles formation can be conducted using UV–Vis spectroscopy as a straightforward technique. In the later sections, more insight into the formation of Cu nanoparticles will be discussed. From impedance data points, one can observe that the high frequency semicircle is resulted from a process associated to the bulk ionic conductivity in the polymer electrolyte. This is due to the migration of the ions in the polymer electrolyte [2]. The centre of the semicircle is located below the x-axis, indicating relaxation time distributions [28, 29]. A straight inclined line at low frequency with a few data points is resulted from electrode polarization (EP) [30]. This phenomenon is related to the fact that ions are accumulated and depleted at each electrode as they move in the alternating field. It is self-evident that each loop is resulted from accumulation of ionic charges at the adjacent region to the electrode, showing the double layer formation. This double layer region leads to the electrode polarization (EP) [31, 32]. The disappearance of the high frequency semicircular region in the impedance plot (see Fig. 1c) has led to a conclusion that the total conductivity is mainly the result of ion migration at higher CuNt salt concentration [10].

3.2 UV–Vis and Impedance Study at Different Temperatures

Figure 2 shows the absorption spectra of the electrolyte samples. A distinguishable broad peak at 702 nm was appeared for all the samples. Ramya et al., have also observed the broad peak at these region for PVA:$Cu(NO_3)_2$ solid electrolytes but they do not give any possible explanation [19]. Cuevvas et al. have studied, however, a peak at around 600–700 nm and ascribed to the copper based nanoparticles formation [33]. Dang et al. have observed comparable broad peaks for Cu nanoparticles [34]. The light absorption by nanoparticles results in a coherent and collective oscillation of electrons. It is well-known that dielectric of the host material impacts the optical properties; in addition to that, the size and shape of the nanoparticles have significantly affected these properties [35]. Sohrabnezhad and Valipour [36], have reported that Cu^{2+} ions with a $3d^9$ electronic configuration shows the d-d transition occurring as a consequence of crystal field induced by ligand-containing hydroxyl in the visible or near-IR range. These bands are due to atomic copper cluster, Plasmon resonance band and octahedral Cu^{2+} ions, respectively [36]. Generally, the use of bio-polymers as stabilizers for the synthesis of Cu-NPs is gaining advancement because of their availability, biocompatibility and low toxicity [37]. It is confirmed that soluble polymers and surfactants, which are used as stabilizers, and also complexing agents are crucial for preventing agglomeration of relatively small nanoparticles [38]. It is obvious from the TEM image (see Fig. 3) that the Cu nanoparticles are finely distributed without aggregation. Copper supported on or incorporated into solid matrices is widely used for preparation of catalysts and nanocomposites with unusual optical, electrical and magnetic properties [39]. Moreover, copper based semiconductors are considered as promising materials in the solar energy conversion into electric and chemical energy due to their small optical band gaps [40]. From the present work, it seems that copper containing solid polymer composites are relatively durable at high temperature. Figure 4 shows the absorption spectra for CSSPE 3 sample at different temperatures. It is clearly seen that the SPR peak at 393 K is comparable to that at room temperature, indicating that no more copper ions undergone reduction to copper nanoparticles throughout the host chitosan solid electrolyte. In our previous work, it was shown that a massive amount of Ag ions undergone reduction to metallic nanaparticle throughout chitosan

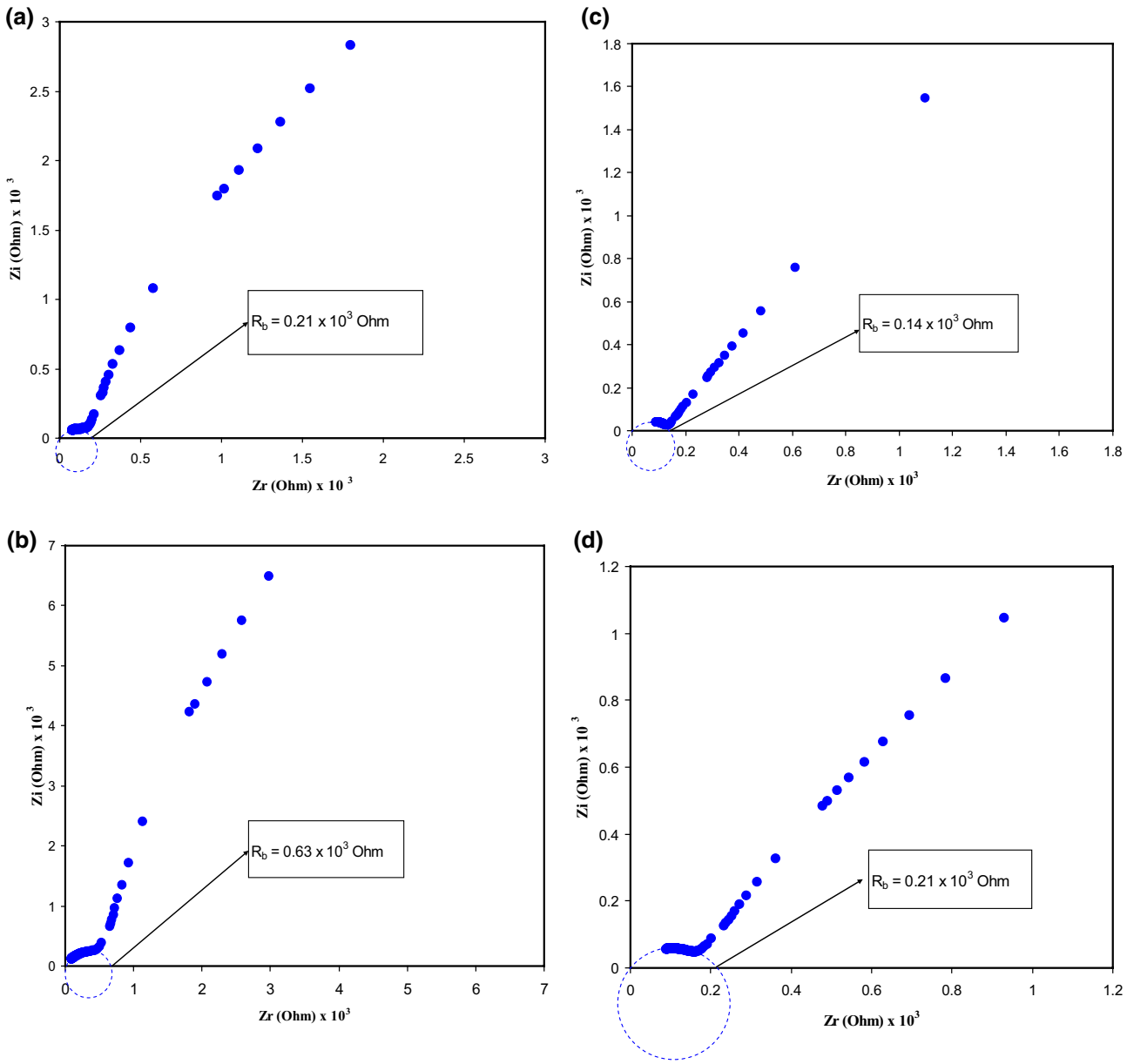

Fig. 1 Impedance plots for **a** CSSPE1, **b** CSSPE 2, **c** CSSPE 3 and **d** CSSPE4 sample

solid electrolyte incorporated with silver triflate (AgTf) salt at high temperature [20, 21, 25]. From the impedance result data, it has also confirmed that the diameter of the second loops increased with increasing temperature as a result of reduction of a high concentration of Ag ion to nanoparticles. Furthermore, from the result data we have noticed a decrease in DC conductivity at 353 K for CS:AgTf system [25]. From the present work, it is shown that the copper-based ion conducting polymer electrolytes are superior to the silver counterparts. For more confirmation, we have studied the impedance plots for CSSPE 2 sample at different temperature as depicted in Fig. 5. It is clear that at 50 °C two semicircles can be distinguished. The second one can be attributed to the reduction process of copper ions to nanoparticles. As the temperature increased, in particular, 90 and 110 °C, only one loop was dominated and the other diminished. The disappearance of second semicircle at high temperatures is an evident for the fact that no more reduction of Cu^{2+} cations occurs and the increase of ionic mobility will increase the DC ionic conductivity and thus a continues drop in bulk resistance will occurs. The results of UV–Vis study at different temperatures presented in Fig. 4 strongly support the fact that at high temperatures reduction of copper cations does not occurs. In our previous works, we observed a big enhancement in SPR peaks of silver nanoparticles at

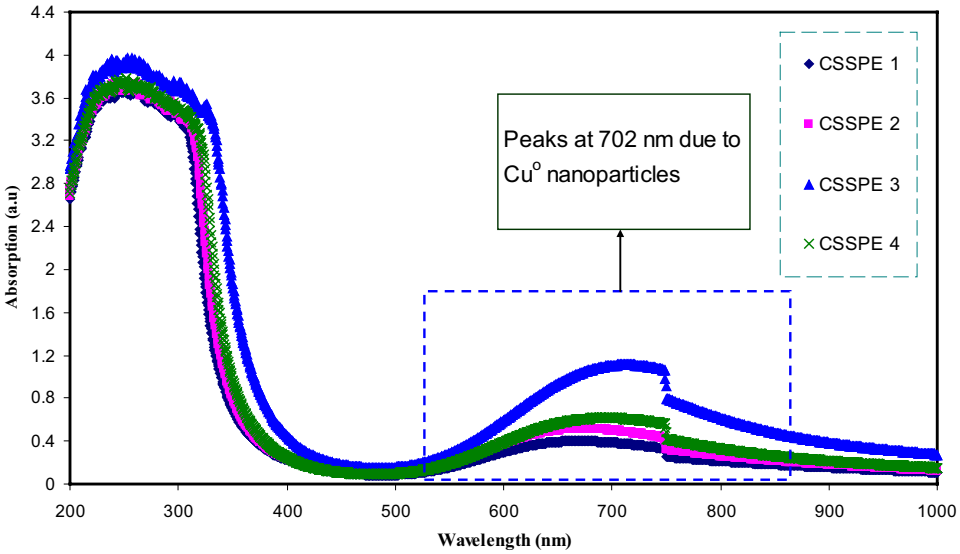

Fig. 2 UV–Vis spectra for all the CS:CuNt solid electrolyte samples at room temperature

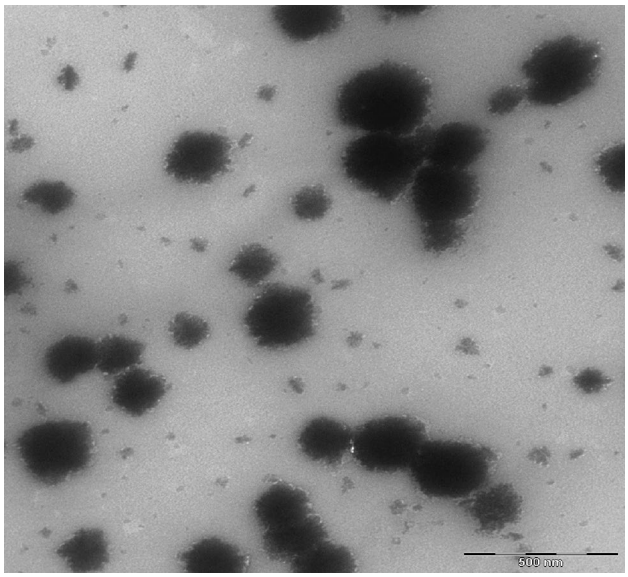

Fig. 3 TEM image for CSSPE3 sample

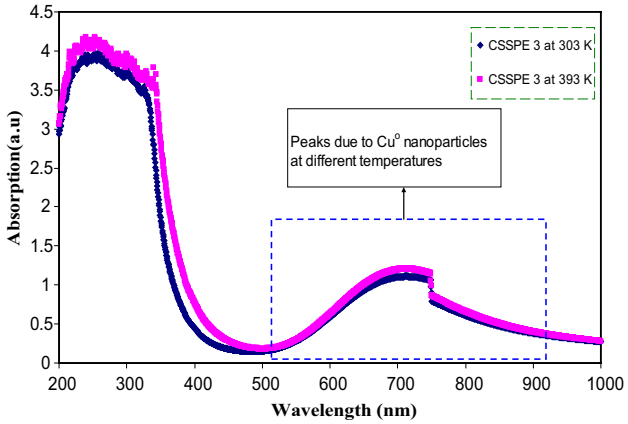

Fig. 4 UV–Vis spectra for CSSPE3 sample at different temperatures temperature

high temperatures [21, 25]. The current study shows that reduction of copper ions as divalent cation in solid state films may not or little occur, which is exactly different to that for silver one as mono-cation.

3.3 Morphological Analysis

To study the morphology, composition and detection of the plasmonic metal nanoparticles, SEM and EDAX are sufficient to be used [8, 20, 22, 23, 41]. Figure 6 shows the morphology of the samples, in which white spots could not be observed on the surface of the samples. However, a distinct white chains and a percolative path were already noticed for the copper nanoparticles in CS:CuI based solid electrolyte films [42]. The white chain formation might be associated to the difference between the sizes of anions of copper salts. Copper salts with larger anions (radius of I = 0.206 nm) result in a much stronger capability to complex with polar groups that have non-bonded electron pair than those with smaller anionic size (radius of NO_3^- = 0.189 nm) [8, 43]. It is well-known that ion reduction process has considerably been influenced by transition metal salts lattice energy [8, 25, 43, 44]. For example, the lattice energy of CuI and Cu $(NO_3)_2$ are 832 and 2720 KJ mol^{-1}, respectively [45, 46]. From electrostatic attraction point of view, the attraction between copper in one side and iodide and nitrate on the other side are completely different. Therefore, stronger attraction can be observed in Cu $(NO_3)_2$ than the iodide salt of copper. It was documented that copper ions in copper iodide are available for reduction compared to the nitrate salt

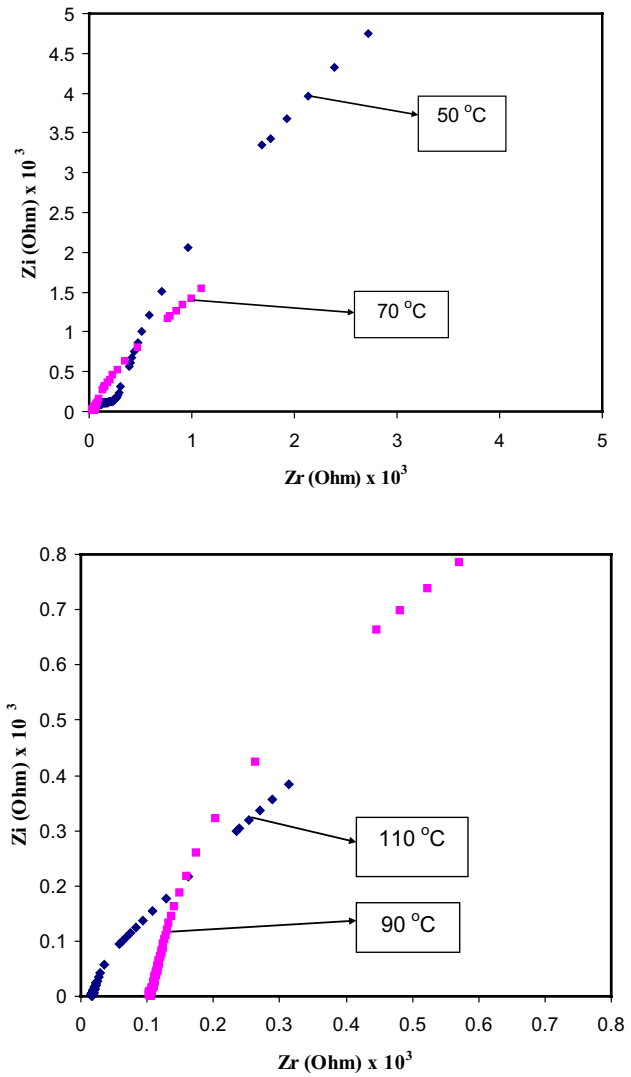

Fig. 5 Impedance plots for CSSPE 2 sample at different temperatures

and white chain was noticed [42]. Likewise, it was observed this phenomenon oppositely for copper nitrate salt in the current work as shown in Fig. 4. The former work has showed that white chain is formed on the AgTf solid electrolyte surfaces, as a result of reduction of massive amount of silver ions to silver nanoparticles [20]. However, we detected very little white spots of silver particles in CS:AgNt solid electrolytes as a result of little reduction of silver ions due to the high lattice energy of AgNt (773 KJ/mol) salt compared to AgTf (716 KJ/mol) salt [8, 44].

3.4 AC Conductivity Study

Figure 7 shows the AC conductivity spectra for all electrolyte samples. From the AC conductivity patterns, one can clearly observe frequency dependent plateau in the frequency region and also dispersion at higher frequency region. These observations follow the universal power law, $\sigma_{(\omega)} = \sigma_{dc} + A\omega^{S}$, where σ_{dc} is the DC conductivity (i.e., frequency independent plateau in the low frequency region), A is the pre-exponential factor and S is the fractional exponent between 0 and 1. The electrode polarization effect is expressed by small deviation from σ_{dc} (i.e., plateau region) value in the conductivity spectrum (i.e., in the low frequency). It was reported that the electrode polarization effect strongly affected by temperature and will shift from low frequency to high frequency regions with increasing temperatures [47]. In general, ionic conductors exhibit power law exponents (S) in the range of 1 and 0.5 for ideal long-range pathways and diffusion limited hopping (twisted pathway), respectively [48]. It is clear from Fig. 8 that the minimum value of S was recorded for CSSPE3 sample. This is related to the high conductivity of CSSPE3 sample. In our previous work, we have established that the dispersion region of AC conductivity is correlated with high frequency semicircles of impedance plots [10]. For the high conducting samples, the semicircle has disappeared as depicted in Fig. 1c and thus a little dispersion regions could be distinguished in AC spectra as depicted in Fig. 7c. The well documented observation revealed that as the conductivity increased, the frequency exponent (s) decreased [10, 20, 29]. For low ionic conductivity system, there is a strong coulomb attraction between the ions and thus wider dispersive region of ac conductivity spectra at higher frequencies, [29], can be seen as depicted in Fig. 7 b. Consequently, a high value of S may be obtained as achieved for 14 wt% CuNt (CSSPE2 sample). Therefore, S value can be used to investigate the conductivity behavior of the samples. The estimated DC conductivity values of the samples are shown in the insets of Fig. 7. This observation is in a good agreement with the bulk resistance values presented in the inset of Fig. 1.

3.5 Dielectric Properties

The dielectric constants versus frequencies for all samples at room temperature are presented in Fig. 9. This study is helpful in dealing with the conductivity property of polymer electrolyte. From this study, one can gain insight into the electrode polarisation effect as a result of electrified region, in the other word, interfacial region between the electrode and electrolyte and also understanding the trend of conductivity [11, 20, 22, 49]. Figure 9 reveals the absence of relaxation peaks, which shows that this increase in conductivity is considerably owing to the increase in number of ion mobility [49]. At low frequency region, the dielectric constant, ε', showed relatively large number as a consequence of dipole alignments with the electric field, conversely, at the high frequency region, the situation is reversed [50]. The ascending ε' values sharply toward low frequency can be resulted from electrode polarization process. It is self-evident that

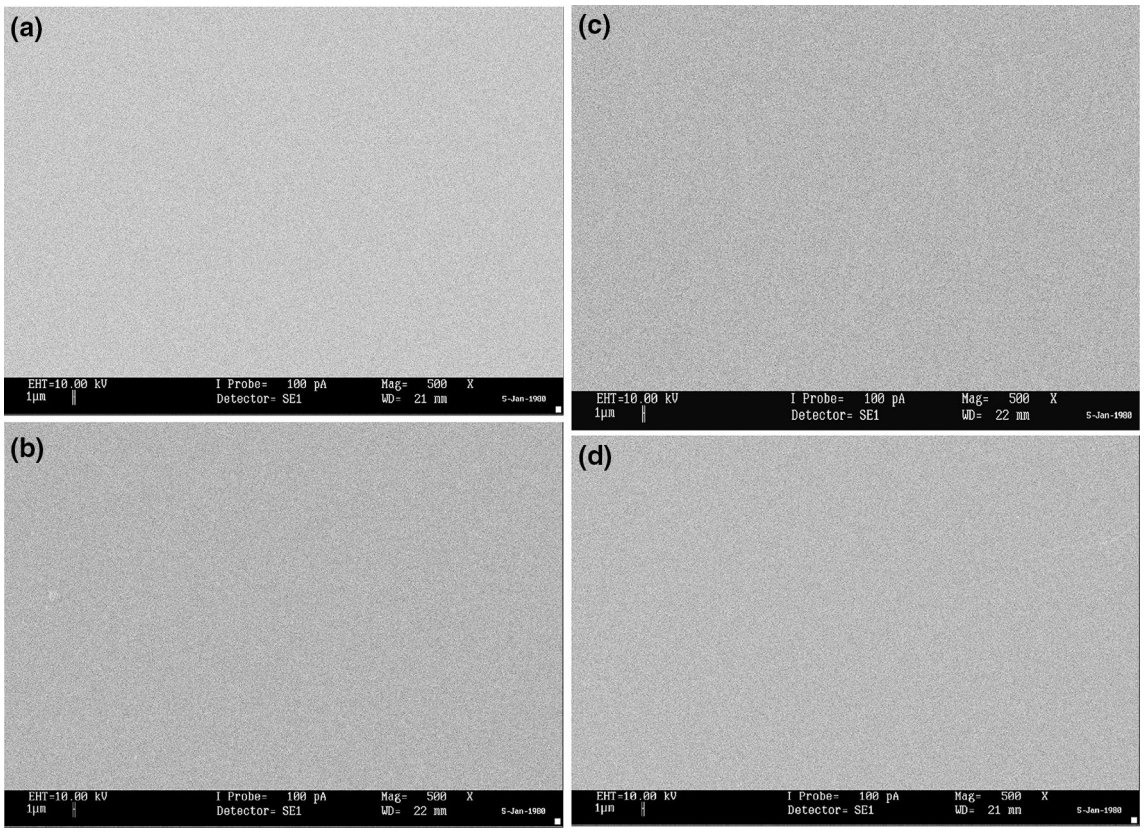

Fig. 6 SEM images for **a** CSSPE1, **b** CSSPE 2, **c** CSSPE 3 and **d** CSSPE4 sample

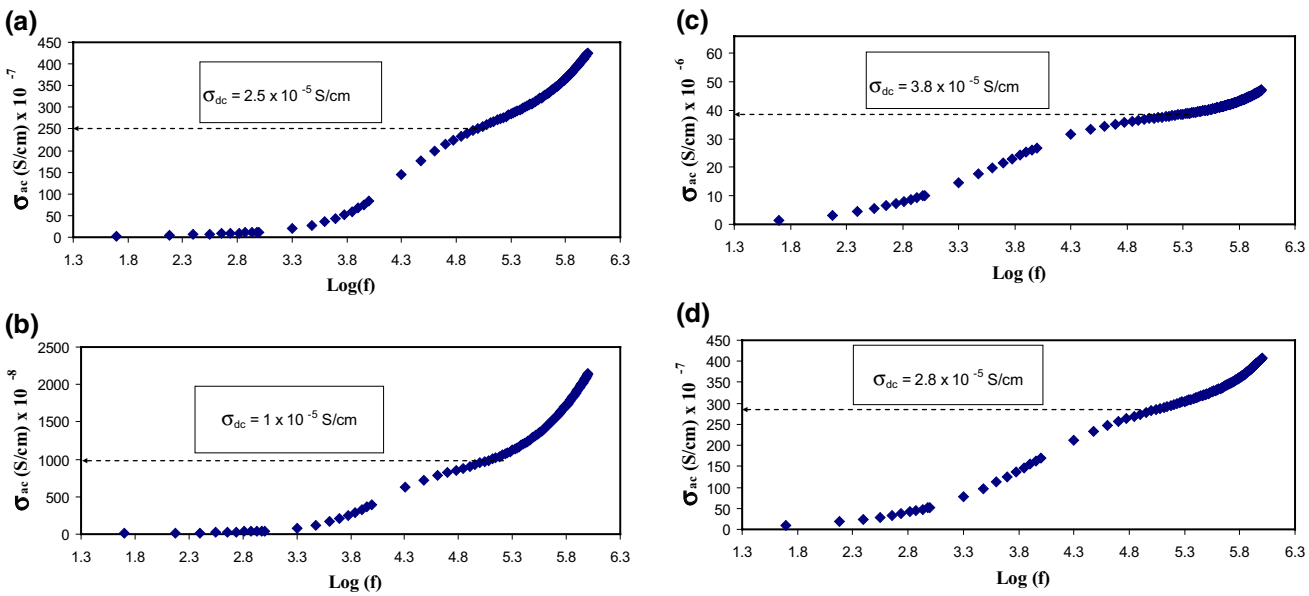

Fig. 7 AC conductivity versus frequency for **a** CSSPE1, **b** CSSPE 2, **c** CSSPE 3 and **d** CSSPE4 sample at room temperature

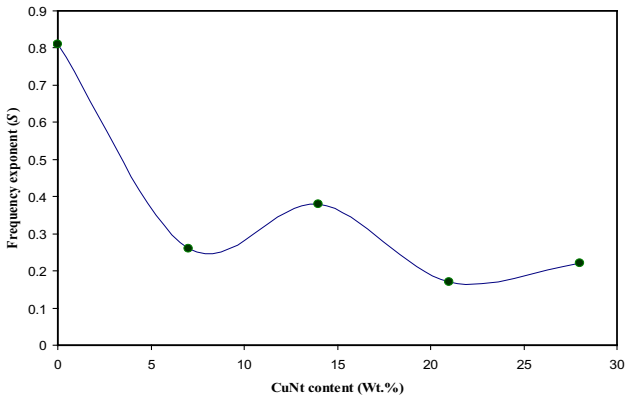

Fig. 8 Frequency exponent (S) versus CuNt concentration at ambient temperature

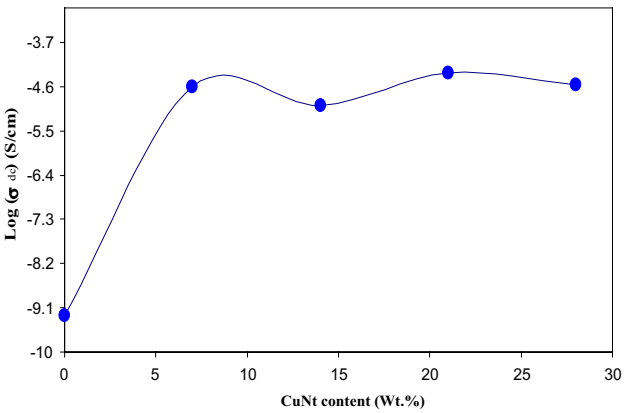

Fig. 11 Room temperature DC conductivity as a function of CuNt salt concentration

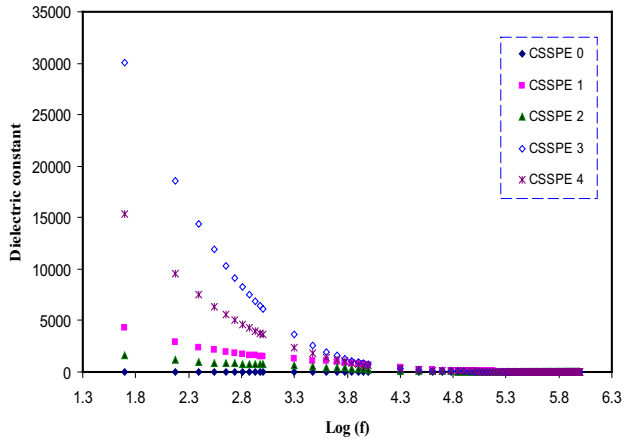

Fig. 9 Dielectric constant versus frequency at room temperature for all the samples

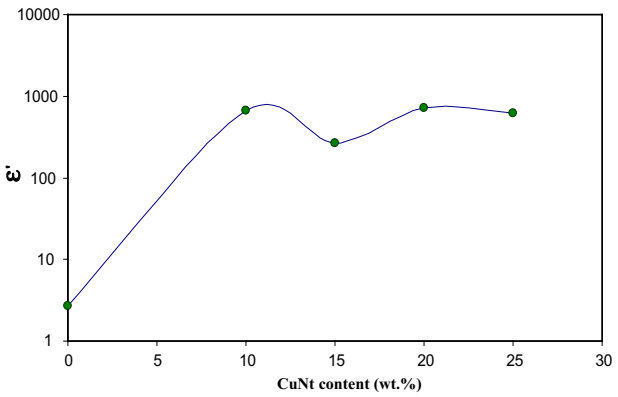

Fig. 10 Dielectric constant (at 10 kHz) versus CuNt salt concentration

charge accumulation at the interfacial region resulted in double layer capacitances. The result data from fast periodic reversal of the electric field at high frequency region has produced absence of polarization. This is due to the incapability of mobile ions to accumulate at the double layer region, leading to the decrease in ε' at high frequency [51]. Figure 10 shows the variation of ε' as a function of salt concentration. This study of dielectric constant versus salt concentration is of significant importance in understanding conductivity of polymer electrolytes [7, 10, 11, 20, 22, 32, 44, 52]. Knowing about the dielectric constant enables physics and chemist researchers to be able in determining the tendency of polymer to solubilizing salts [53]. Figure 11 shows clearly the DC conductivity versus salt concentration. It is worth noting that both DC conductivity and ε' versus salt concentrations are comparable. This is predictable because both DC conductivity ($\sigma_{dc} = q\mu n$) and dielectric constant ($n = n_o\ exp^{(-U/\varepsilon' KBT)}$) are charge carrier density dependent [7, 11, 22]. Thus, from the study of dielectric constant, the conductivity behavior of the samples can be understood. It is obviously noticed that as the concentration is increased to 14 wt% CuNP, the conductivity has decreased due to the formation of ion pair. At 21 wt% CuNP, however, the conductivity has increased again, which can be ascribed to triple ion formation or re-dissociation process. Ultimately, the study has continued using higher concentration of 28 wt% CuNP and a decrease in conductivity was observed, which might be owing to either rapid increase in viscosity [11] or higher ion aggregation, as a result, the film flexibility is decreased [54].

To represent analyzing ionic conductivities in dealing with relationship between conductivity relaxation time and ionic process, M^* is denoted [47]. Figure 12 shows the Argand plots for all samples. Relaxation phenomena can be interpreted using electric modulus formalism that provide several advantages, such as permittivity and conductivity relaxation treatments, due to that large variation in the ε'

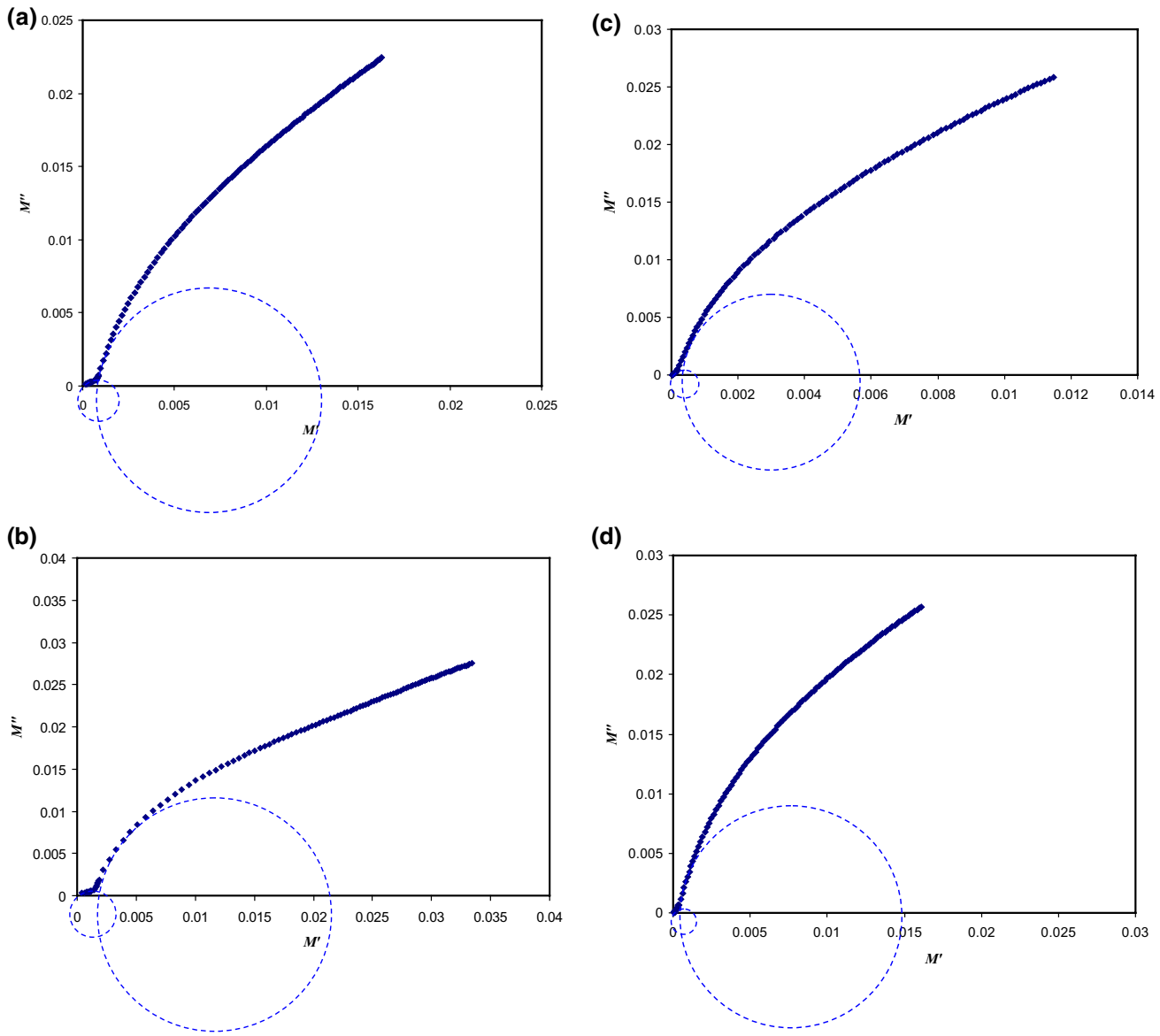

Fig. 12 Argand plots for **a** CSSPE1, **b** CSSPE 2, **c** CSSPE 3 and **d** CSSPE4 sample

and ε'' values are minimized at low frequency and high temperature. Furthermore, difficulties occurring in the analysis of dielectric spectra from the electrode nature (electrode material), the electrode specimen electrical contact and the injection of space charges with absorbed impurities can be neglected [55]. The two loops are separable at low and high frequency regions. The non-Debye type relaxation process can be identified from incomplete semicircle as shown in the Argand plots. The Debye model is developed to noninteracting identical dipoles [56]. The appearance and separation of two semicircles clearly are related to the fact that in electric modulus study the effects due to electrode polarization can be minimized. The second loop in Argand plots could be attributed to electronic contribution.

4 Conclusions

In conclusion, it seems strongly from impedance plots and UV–Vis spectroscopy that copper nanoparticles are formed. The curvature observed in impedance plots at intermediated frequencies can be regarded as second semicircles in impedance plots. The broad surface plasmonic resonance (SPR) peaks at 702 nm reveals the formation of copper particles with nano sizes. The Cu nanopartciles are sources for electronic conductivity in CS:CuNt based polymer electrolytes. The appearance of second semicircles in impedance plots satisfies the contribution of electronic conductivity in CS:CuNt based ion conductors. The thermally stability of CS:CuNt based polymer electrolytes could be concluded

from the unchanged shape and intensity of UV–Vis spectra at different temperatures. The stable SPR peak and vanishing of second semicircle at high temperatures reveal the stability of copper ion conducting chitosan solid electrolytes. The high lattice energy of CuNt salt is responsible for the smooth surface (SEM) of the samples. The TEM image shows the distribution of Cu nanoparticles with various sizes. The existing of electronic conductivity in CS:CuNt based electrolytes can be considered as the main shortcoming of copper ion conducting based solid polymer electrolytes. Similar trends of DC conductivity and dielectric constant versus salt concentration are helpful for understanding the conductivity behavior of polymer electrolytes. The estimated DC conductivity from AC spectra is close enough to those calculated from the impedance plots. The highest DC conductivity of 3.65×10^{-5} S/cm was achieved for the sample incorporated 20 wt% CuNt. The high value of dielectric constant at low frequency can be ascribed to electrode polarization. The incomplete semicircular arcs with diameter located below the real axis reveals that relaxation processes follows the non Debye type relaxation. The second semicircle in Argand plots could be ascribed to electronic contribution.

Acknowledgements The author gratefully acknowledge the financial support for this study from Ministry of Higher Education and Scientific Research-Kurdistan Regional Government, Department of Physics, College of Science, University of Sulaimani, Sulaimani, and Komar Research Center (KRC), Komar University of Science and Technology, Sulaimani, 46001, Kurdistan Regional Government, Iraq.

References

1. S.B. Aziz, O.G. Abdullah, M.A. Rasheed, H.M. Ahmed, Polymers **9**, 187 (2017)
2. K. Sownthari, S.A. Suthanthiraraj, Express Polym. Lett **7**, 4956 (2013)
3. N.K. Idris, N.A. Nik Aziz, M.S.M. Zambri, N.A. Zakaria, M.I.N. Isa, Ionics **15**, 643 (2009)
4. L. Caoab, M. Yangab, D. Wua, F. Lyua, Z. Suna, X. Zhongab, H. Panb, H. Liuc, Z. Lu, Chem. Commun. **53**, 1615 (2017)
5. M.F. Shukur, Y.M. Yusof, S.M.M. Zawawi, H.A. Illias, M.F.Z. Kadir, Phys. Scr. **2013**(T157), 014050 (2013)
6. M.N. Chai, M.I.N. Isa, Sci. Rep. **6**, 27328 (2016)
7. N.S. Salleh, S.B. Aziz, Z. Aspanut, M. F. Z. Kadir, Ionics **22**, 2157 (2016)
8. S.B. Aziz, Z.H.Z. Abidin, J. Soft Mater. **2013** (2013), Article ID 323868
9. S.B. Aziz, O. Gh. Abdullah, D.R. Saber, M.A. Rasheed, H.M. Ahmed, Int. J. Electrochem. Sci. **12**, 363 (2017)
10. S.B. Aziz, Z.H.Z. Abidin, J. Appl. Polym. Sci. **132**, 41774 (2015)
11. S.B. Aziz, M.F.Z. Kadir, Z.H.Z. Abidin, Int. J. Electrochem. Sci. **11**, 9228 (2016)
12. K. Sakurai, T. Maegawa, T. Takahashi, Polymer **41**, 7051 (2000)
13. B. Balakrishnan, R. Banerjee, Chem. Rev. **111**, 4453 (2011)
14. S.V. Vlierberghe, P. Dubruel, E. Schacht, Biomacromol **12**, 1387 (2011)
15. Z. Sun, F. Lv, L. Cao, L. Liu, Y. Zhang, Z. Lu, Angew. Chem. **127**, 8055 (2015)
16. S.R. Majida, A.K. Arof, Polym. Adv. Technol. **20**, 524 (2009)
17. T.B. Sahu, M. Sahu, S. Karan, Y.K. Mahipal, D.K. Sahu, R.C. Agrawal, J. Phys. D **50**, 275501 (2017)
18. K. Perera, M.A.K.L. Dissanayake, P.W.S.K. Bandaranayake, Electrochim. Acta **45**, 1361 (2000)
19. C.S. Ramya, T. Savitha, S. Selvasekarapandian, G. Hirankumar, Ionics **11**, 436 (2005)
20. S.B. Aziz, Z.H.Z. Abidin, Mater. Chem. Phys. **144**, 280 (2014)
21. S.B. Aziz, Z.H.Z. Abidin, A.K. Arof, Express Polym. Lett. **4**, 300 (2010)
22. S.B. Aziz, O. Gh., M.A. Abdullah, Rasheed, J. Appl. Polym. Sci. **134**, 44847 (2017)
23. S.B. Aziz, Z.H.Z. Abidin, M.F.Z. Kadir, Phys. Scr. **90**, 035808 (2015)
24. S.B. Aziz, M.A. Rasheed, Z.H.Z. Abidin, J. Electron. Mater. **46**, 6119 (2017)
25. S.B. Aziz, Z.H.Z. Abidin, A.K. Arof, Phys. B **405**, 4429 (2010)
26. G.B. Patel, N.L. Singh, F. Singh, Mater. Sci. Eng. B **225**, 150 (2017)
27. S.B. Aziz, S.M. Mamand, S.R. Saed, R.M. Abdullah, S.A. Hussein, J. Nanomater. **2017** Article ID 8140693 (2017)
28. S.B. Aziz, Bull. Mater. Sci. **38**, 1597 (2015)
29. S.B. Aziz, Appl. Phys. A **122**, 706 (2016)
30. C.R. Mariappan, G. Govindaraj, Mater. Sci. Eng. B **94**, 82 (2002)
31. A.M. Stephan, R. Thirunakaran, N.G. Renganathan, V. Sundaram, S. Pitchumani, N. Muniyandi, R. Gangadharan, P. Ramamoorthy, J. Power Sources **81– 82**, 752 (1999)
32. S.B. Aziz, R.M. Abdullah, M.A. Rasheed, H.M. Ahmed, Polymers **9**, 338 (2017)
33. R. Cuevas, N. Durán, M.C. Diez, G.R. Tortella, O. Rubilar, J. Nanomater. **2015** (2015), Article ID 789089
34. T.M.D. Dang, T.T.T. Le, E. Fribourg-Blanc, M.C. Dang, Adv. Nat. Sci. **2**, 015009 (2011)
35. J.M.P. Almeida, L. De Boni, W. Avansi, C. Ribeiro, E. Longo, A.C. Hernandes, C.R. Mendonca, Opt. Express **20**, 15106 (2012)
36. A. Sohrabnezhad, A. Valipour, Spectrochim. Acta Part A **114**, 298 (2013)
37. M.S. Usman, N.A. Ibrahim, K. Shameli, N. Zainuddin, W.M.Z.W. Yunus, Molecules **17**, 14928 (2012)
38. E. Alzahrani, R.A. Ahmed, Int. J. Electrochem. Sci. **11**, 4712 (2016)
39. A.N. Pestryakov, V.P. Petranovskii, A. Kryazhov, O. Ozhereliev, A. Knop-Gericke, Chem. Phys. Lett. **385**, 173 (2004)
40. M. Salavati-Niasari, F. Davar, Mater. Lett. **63**, 441 (2009)
41. D. Wei, W. Sun, W. Qian, Y. Ye, X. Ma, Carbohydr. Res. **344**, 2375 (2009)
42. S.B. Aziz, Nanomaterials **7**, 444 (2017). https://doi.org/10.3390/nano7120444
43. S. Hong, C.K. Kim, Y.S. Kang, Macromolecules **33**, 7918 (2000)
44. S.B. Aziz, O.Gh. Abdullah, S.A. Hussein, J. Electron. Mater. (2018). https://doi.org/10.1007/s11664-018-6250-5
45. J.E. Mayer, R.B. Levy, J. Chem. Phys. **1**, 647 (1933). https://doi.org/10.1063/1.1749345
46. C.H. Yoder, N.J. Flora, Am. Mineral. **90**, 488 (2005)
47. D.K. Pradhan, R.N.P. Choudhary, B.K. Samantaray, Express Polym. Lett. **2**, 630 (2008)
48. D.K. Pradhan, R.N.P. Choudhary, B.K. Samantaray, Int. J. Electrochem. Sci. **3**, 597 (2008)
49. A.A. Azli, N.S.A. Manan, M.F.Z. Kadir, Adv. Mater. Sci. Eng. **2015** (2015), Article ID 145735

50. N. Kulshrestha, B. Chatterjee, P.N. Gupta, High Perform. Polym. **26**, 677 (2014)
51. C.-S. Lim, K.H. Teoh, H.M. Ng, C.-W. Liew, S. Ramesh, Adv. Mater. Lett. **8**, 465 (2017)
52. S.B. Aziz, O.G. Abdullah, S.A. Hussein, H.M. Ahmed, Polymers **9**, 622 (2017). https://doi.org/10.3390/polym9110622
53. W. Wang, P. Alexandridis, Polymers **8**, 387 (2016). https://doi.org/10.3390/polym8110387
54. M. Hema, S. Selvasekarapandian, D. Arunkumar, A. Sakunthala, H. Nithya, J. Non-Cryst. Solids **355**, 84 (2009)
55. R.J. Sengwa, S. Choudhary, Express Polym. Lett. **4**, 559 (2010)
56. S.B. Aziz, Adv. Mater. Sci. Eng. **2016** Article ID 2527013 (2016)